MRS Advances
https://doi.org/10.1557/s43580-024-00804-5

ORIGINAL PAPER

Controlling reaction transfer between Al/Ni reactive multilayer elements on substrates

Deepshikha Shekhawat[1] · Muhammad Sulman[1] · Manuela Breiter[2] · Jörg Pezoldt[1]

Received: 25 November 2023 / Accepted: 8 February 2024

Abstract
Reactive multilayers produce exothermic reaction with definite velocity and maximum temperature after ignition, which are the fundamental properties of the reactive multilayer systems. The generated heat with certain velocity makes it widely used in joining, bonding in the packaging, thermal batteries and many more applications. In this work, a distinct approach for achieving a reaction transfer between the reactive multilayers and different materials is demonstrated which can affect the generated temperature and velocity from the self-propagating properties of the reaction. For these intensions, we fabricated the Al/Ni reactive elements with certain separations between elements which allow to observe the reaction front transfer and emitted temperature in the reaction chain. The created separation between reactive elements are periodical and ordered systems with different thermal conductive properties. The temperature and definite velocity were measured by time-resolved pyrometer and high-speed camera measurements. SEM analysis showed the characteristics of the reaction transfer between reactive multilayer elements. It is predicted that: (I) The reaction front stops at a space with critical length; (II) Reducing heat loss through the substrate supports reaction front propagation through spaces; (III) Thermal property design of the spaces between the reactive elements enables property modification of the self-propagating reaction.

Introduction

During the last decade, reactive multilayer films have attracted attention of the researchers due to its highly exothermic reaction which can be used as a heat source in low-temperature soldering and bonding in the packaging of microsystems applications [1, 2]. Self-propagating reaction can be perceived by enough heat released from local mixing to heat the adjacent material and brought a self-sustaining reaction front which moves forward through the reactive multilayers with a typical temperature and velocity [1–3]. The uses of integrated reactive multilayer systems in microelectronics and micromechanical systems (MEMS) as a bonding material technique has lately gained more traction and attention [4–9]. Therefore, integration processing by the patterning or deposition of reactive films directly on silicon or other substrate is an interesting research challenge. Since, properties of the reactive multilayers are not only dependent on the properties of the reactive materials but also influenced by the properties of substrate materials such as thermal conductivity, heat capacity and density on the characteristics of the reaction of the foils [10]. It was observed that increased thermal conductivity of the substrate material can decreases the maximum temperature of the reaction and can ultimately causes the reaction to quench. Effect of heat capacity and density of the substrate material are found to be insignificant effect on the properties of the reaction, although in critical cases, can origin the quenching of the reaction. Heat generates after an initial ignition source by electric spark, laser or mechanical force creates a self-propagating exothermic reaction of the integrated reactive multilayer systems [7, 8, 11, 12]. The reactive integrated bond induces local heat to bond the interface. Such limited temperature source may be quenched locally over heat sinks existing on or in the substrate material. The interaction of disconnected reactive material reservoirs was investigated for explosion transfer protection [13, 14], stability issues in flame propagation

✉ Deepshikha Shekhawat
deepshikha.shekhawat@tu-ilmenau.de

✉ Jörg Pezoldt
joerg.pezoldt@tu-ilmenau.de

[1] FG Nanotechnologie, Institut für Mikro- und Nanolektronik and Institut für Mikro- und Nanotechnologien MacroNano® and Institut für Werkstofftechnik, TU Ilmenau, Postfach 100565, 98684 Ilmenau, Germany

[2] Zentrum für Mikro- und Nanotechnologien, TU Ilmenau, Postfach 100565, 98684 Ilmenau, Germany

Published online: 26 February 2024

[15–18], reaction delay times in self-propagating reactions[19, 20]. Most of this research was based on reactive elements and obstacles with macroscopic dimensions.

The purpose of this investigation is to experimentally downscale the reactive material elements and the obstacles to microscale dimensions and see the effects of the separation between reactive material elements and the different thermal conductive materials filling the separations between Al/Ni reactive material blocks on a Si/SiO_2 substrates. As a model system Ni/Al multilayer films with a 50 nm bilayer thickness (atomic ratio of Al to Ni is 1:1) was deposited by DC source magnetron sputtering on a patterned Si/SiO_2 substrates. The influence of Ni/Al total thickness, the separation distances and heat loss conditions on self-propagating exothermic reaction in structured heterogeneous multilayer reactive material systems are investigated and discussed.

Materials and experimental techniques

Si (100) p-type doped; 1 µm wet oxidized SiO_2 on top of p-type Si (SiO_2/Si) is used for fabrication as shown in Fig. 1. Initially, sample organic cleaned with Acetone, Iso-propanol alcohol and deionize water to remove the residual impurities present in Si/SiO_2 substrate. Substrates were placed at 105 °C temperature for 30 min to remove the excess water from the surface of the substrates, the HMDS coating was done at 90 °C for 1 min. We used three types of resist. For Sample A and Sample B: AZ1518; for Sample C, Sample D and Sample E: AZ15nxt; Sample F and Sample G: AZ 3027 to get 3.8, 10 and 3.1 µm thickness of the resist. Then resist coated substrates were exposed with the help of photolithography tool. Deep reactive ion etching was also done in sample F and sample G to etch Si substrates with the inductively coupled plasma (ICP) Pro Estrday 100 for 3.5 min to make 15 µm deep etching into the Si substrates. After etching, liftoff was done in MLO07 Technistripper for 11 min. Then followed by, Ni and Al deposited by DC magnetron sputtering (CS400 by von Ardenne), where Ni and Al (99.99% purity, FHR) with 100 mm diameter targets were used. Alternating layers of 20 nm Ni and 30 nm Al layers thicknesses (50 nm bilayer thickness) were deposited by magnetron sputtering. Depositions were performed at room temperature at a base pressure of $5 \times 10 - 8$ Torr. Final a series of samples are prepared and summaries in Fig. 1. A 16 V electrical spark was used for the ignition of reactive multilayers. The electrical probes were placed at the edge of the fabricated sample. High-speed camera (FASTCAM SA-X2) with a 50,000 fps frame rates were used to record the front velocity of the self/propagating reaction. The high-speed pyrometer (KLEIRER—Pyroscope 840 pyrometer) was used to measure reaction temperature with an emissions coefficient (ε) value fixed to 1 with 10 µs resolution time. The recorded temperature was corrected after the measurements using the emission coefficient determined in separate experiments. To explore the microstructural features on the top of the deposited reactive Ni/Al multilayers on Si/SiO_2 substrates, using SEM (S-4800 HITACHI) for before and after the reaction. The phase identification of the reacted and unreacted Al/Ni chips were obtained from X-ray diffraction (XRD) Bruker D5000 Theta-Theta X-ray diffractometer with Cu-Kα (1.5406 A) radiation at 40 mA and 40 kV with Bragg–Brentano working mode.

Results and discussion

To investigate the effects of the separation of different thermal conductive materials between reactive material elements to microscale dimensions, we fabricated chiplets with integrated microstructure reactive Al/Ni elements. Figure 1a and b are the top and side view of the fabricated samples to analyze the self-propagation transfer condition between adjacent Al/Ni reactive materials elements where, Al/Ni reactive materials act as local heat source separated by different thermal conductive materials.

The prepared test chip includes an ignition pad allowing for two ignition points for spark ignition. The squared

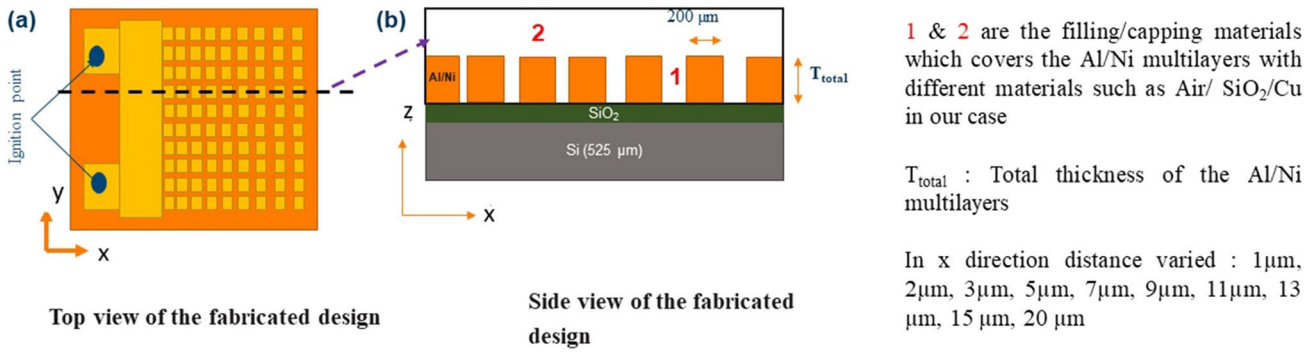

Fig. 1 **a** Is the top view of the prepared samples and **b** is the enlarged cross-section image

reactive material elements had a side length of 200 µm. The distance between these elements was increasing with increasing distance from the ignition pad. The change in the distance series was the following: 1 µm, 2 µm, 3 µm, 5 µm, 7 µm, 9 µm, 11 µm, 13 µm, 15 µm, 20 µm. Three consecutive rows of elements had the same spacing. 1 and 2 in Fig. 1 are filling/capping materials which separates the adjacent Al/Ni multilayers from the different thermal conductive materials. Table 1 shows the summary of the prepared samples. Figure 2 shows the microscopic images of the prepared reactive material elements before and after the ignition of the prepared sample A and sample B. Figure 2a and b are the before and after the reaction on sample A where T_{total} (total thickness of the Al/Ni multilayers) 500 nm Al/Ni. As we can see in Fig. 2a, the minimum spaces between the two adjacent Al/Ni multilayers element is 1 µm. It means, after ignite the reactive multilayers, reaction front moves from one Al/Ni element to other, starts passing over 1 µm spaces between them. We performed ignition experiment, Fig. 2b as we can see, no self-propagation reaction was observed. On the other hand, Fig. 2b showed the effect of the electric spark which was used to ignite the ignition pad, but heat of Al/Ni multilayers couldn't propagate further through the separation. Resultant, we increased the total thickness to 1 µm Al/Ni multilayers. Figure 2c and d are the sample B where T_{total} 1 µm Al/Ni. As we can see in Fig. 2c, we prepared 1 µm structured Al/Ni multilayers on Si/SiO_2 substrate, and we achieved 1 µm minimum spaces between the two adjacent Al/Ni multilayers element. We performed ignition experiment, as we can see in Fig. 2d, no self-propagation reaction was observed with 1 µm total thickness of Al/Ni multilayers on Si/SiO_2 substrate. Figure 2d microscopic images where it showed the thermal effect of the electric spark only on the prepared sample and there is no evidence for further propagation of the heat.

Table 1 Summary of the prepared samples

Samples	Substrates	T_{Total} of deposited Al/Ni multilayer	Filling materials	Capping materials
Sample A	1 µm SiO_2; 525 µm Si	500 nm	Air	Air
Sample B	1 µm SiO_2; 525 µm Si	1 µm	Air	Air
Sample C	1 µm SiO_2; 525 µm Si	5 µm	Air	Air
Sample D	1 µm SiO_2; 525 µm Si	5 µm	500 nm Cu	500 nm Cu
Sample E	1 µm SiO_2; 525 µm Si	5 µm	1 µm SiO_2	1 µm SiO_2
Sample F	1 µm SiO_2; 525 µm Si	5 µm	15 µm Si; 1 µm SiO_2	Air
Sample G	1 µm SiO_2; 525 µm Si	5 µm	15 µm Si; 1 µm SiO_2; 1 µm PMMA	Air

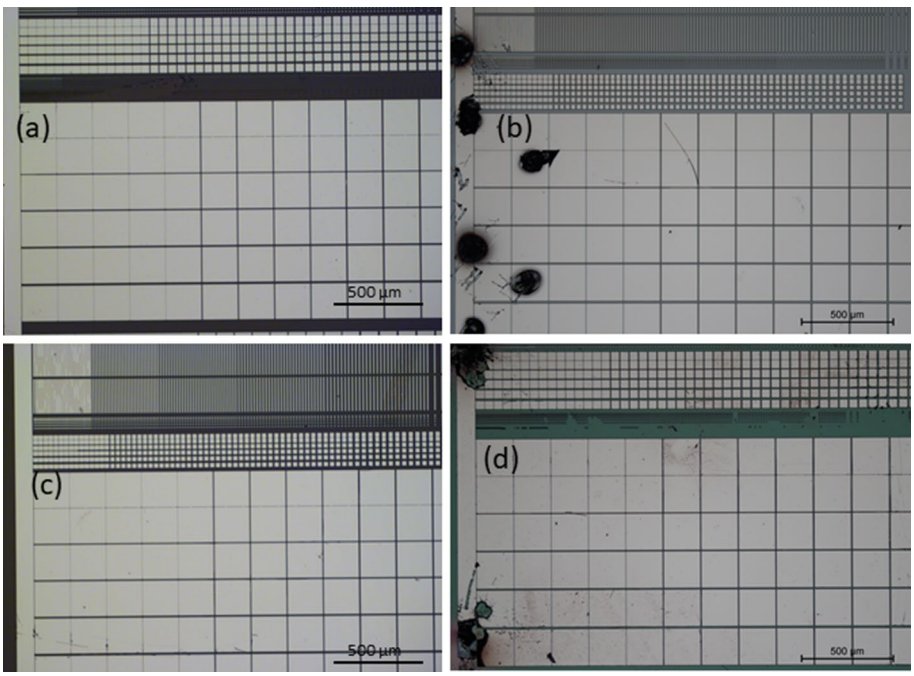

Fig. 2 Microscopic images: **a** before ignition and **b** after ignition for the sample A where T_{total} 500 nm Al/Ni. **c** Before ignition and **d** after ignition for sample B where T_{total} 1 µm Al/Ni

It is reported that to have self- propagation reaction from reactive materials, the heat released by local mixing reaction in the multilayers should be higher than the heat loss through the surrounding area [21].

In addition, the heat balances play an important role in reactive materials to control the self-propagating reaction. The critical condition for not having a self-propagating reaction, is when the heat generation rate equals or lower than the heat loss rate [22]. Overall, the increased heat loss rate from the substrate and surrounding reduces the propagation velocity and the maximum reaction temperature [23–26], if the critical condition is reached, reaction quenching occurs. As a consequence, critical thickness [23–25, 27] of Al/Ni films on Si/SiO_2 substrate is 5 µm [26, 28].

Therefore, we started to prepare the structure with the help of photolithography to deposit 5 µm total thickness Al/Ni multilayers. Since, total thickness of the deposition has been increased, limitation to achieve the minimum separation resolution of the prepared structure is also affecting. Photolithography parameter and optimized parameters have already been demonstrated in the materials and experimental techniques section. Figure 3a shows the SEM image of the prepared samples along with the cross section schematic diagram, where minimum separation was achieved is 10 µm. The changes in the separation series were following: 10 µm, 15 µm, 20 µm and 25 µm. Figure 3b shows the SEM images of prepared sample C, 5 µm structured Al/Ni multilayers, as we can see the minimum spaces between the two adjacent Al/Ni multilayers element is 10 µm. As we can see from Fig. 3b, the reaction front stop at the first separation which is 10 µm. This 10 µm spaces between the Al/Ni element, is too much space to heat the next element. However, due to limitation in the point of photolithography with such thick resist it is difficult to achieve less than 10 µm spaces with these parameters between adjacent Al/Ni element. A possible solution is the increase of the thermal conductivity of the separation by filling the separation with higher thermal conductive materials, which could increase the chance to ignite the next Al/Ni element.

Therefore, we covered 5 µm structured Al/Ni multilayers by Cu (500 nm) and SiO_2 (1 µm)]. Cu and SiO_2 would connect the spaces and cover the whole structured Al/Ni multilayers as shown in the schematic diagram in Fig. 3c–f. After the ignition experiment, we observed sample D and

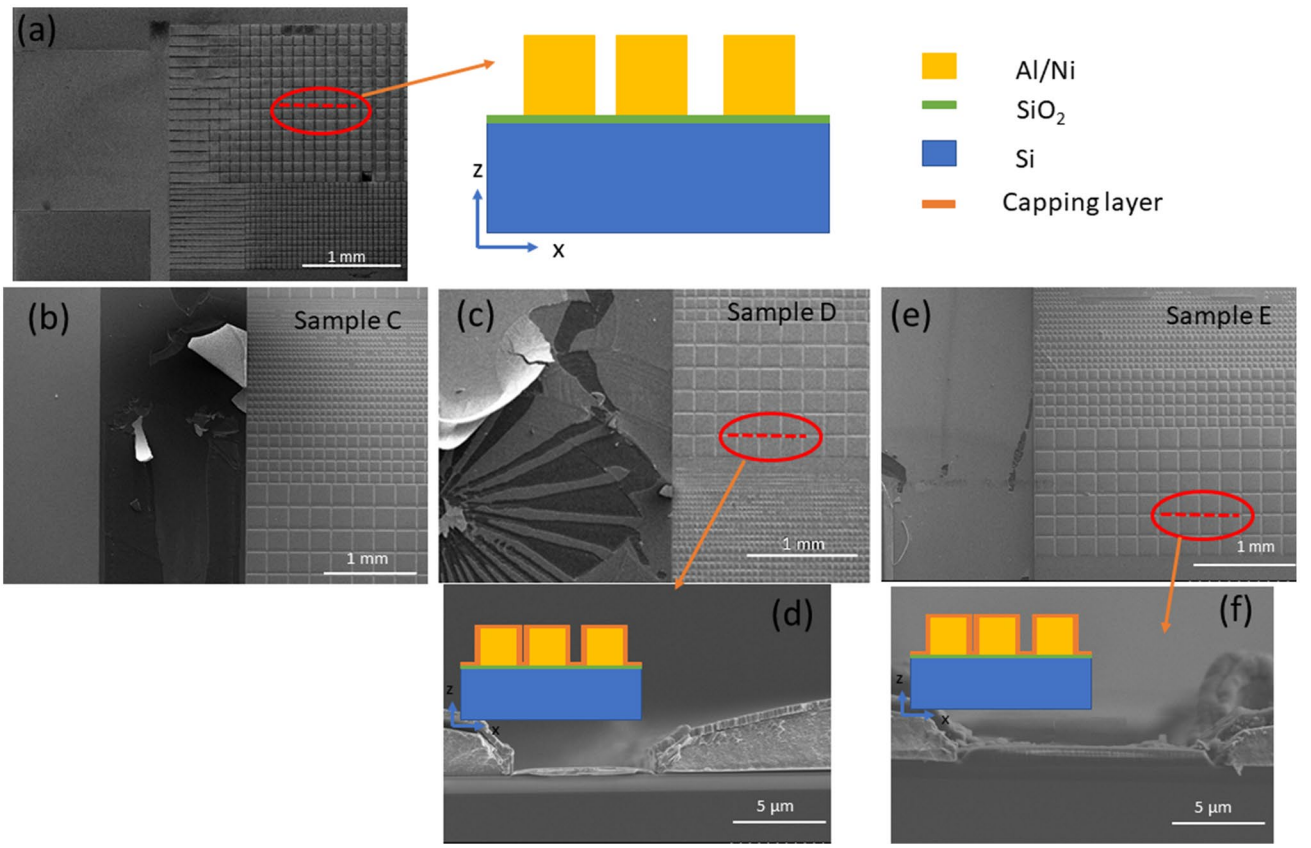

Fig. 3 **a** is the top view SEM image with cross section schematic view of the prepared sample C where, T_{total} 5 µm Al/Ni. **b** is the SEM image of sample C after ignition. **c** is the SEM image of sample D after ignition with cross section image of prepared sample D in **d**. **e** is the SEM image of sample E after ignition with cross section image of prepared sample E in (**f**).is the

sample E, i.e. 500 nm Cu, and 1 μm SiO_2 as capping layer shown in Fig. 3c and e it stopped at the first separation. It may be due to the critical condition reached, where the heat generation rate equals the heat loss rate from the surrounding 10 μm space [13]. Generally, the increased heat loss rate reduces the maximum reaction temperature to heat the next element [14–17], if the critical condition is reached reaction gets quenched.

To overcome the limitation of 10 μm separation, we can achieve the less separation thickness by preparing our structured 5 μm Al/Ni multilayers with the help of dry etching of the respective substrate. Dry etching of Si of 15 μm deep reactive ion etching parameters has been described in materials and experimental techniques. Minimum resolution was achieved by this method is 3 μm width of the separation wall after Al/Ni deposition. The change in the distance series were as follows: 3 μm, 5 μm, 7 μm, 9 μm, 11 μm, 13 μm, 15 μm, 20 μm. Three consecutive rows of elements had the same spacing.

Figure 4a, is the microscopy image of the sample F before reaction. We performed ignition experiment, no self-propagation reaction was observed. However, near to the ignition zone we found reaction affected zone as we can see in Fig. 4c which shows the reaction transfer possible from one reactive material element through a separation material to the next reactive material element due to heat affected region in the attached SEM image. Although, the separation was created due to the side wall of etching process therefore thickness of the wall increased. In Fig. 4c, shows the cross-sectional view after the reaction where reaction stopped to move forward. Since, we couldn't get the self-propagation reaction on the prepared sample. The heat balances in reactive materials play an important role to have self-propagating reaction. The important condition for a self-propagating reaction, is when the heat generation rate is larger than the heat loss rate [22]. So as reported in the [26, 28] PMMA or resist which has lower thermal conductivity can modify the heat loss condition. Since it is reported PMMA has lower thermal conductivity than Si/SiO_2, can reduce the thermal heat loss during the ignition experiment [26]. So, we coated PMMA as a resist by 1 μm thick on the prepared structured Si/SiO_2 substrate. Figure 4b shows the as deposited sample G. We performed ignition experiment, and observed the self-propagation reaction through the whole sample as shown in Fig. 4d. Figure 4d shows the deformation after the reaction which is due to the lattice deformation in the order of 20% due to stress change from unreacted to reacted Al/Ni multilayers. As in Fig. 1, mentioned separation between Al/Ni elements in x- direction. So, from the ignition experiment, reaction front moves from the separation up to 20 μm with sample G system. Finally, we successfully achieved the self-propagation reaction through the different thermal conductive separation. The observed reaction front velocity of the sample G is 10.05 m/s and the maximum temperature was 1083 °C. The measured parameters are lower than the free standing 5 μm Al/Ni multilayer foil which is 11.18 m/s and 1169.6 °C. This difference occurred due to thermal heat loss through the substrates and the separated walls in the sample G. Figure 4e shows the XRD pattern of unreacted and reacted Sample G. It shows in unreacted sample G, Al (PDF 01-1180) and Ni (PDF 65-2865) were present. After the reaction, it demonstrated the crystallized B2 AlNi (PDF 65-5171) phase formation from elemental Ni and Al phases from unreacted samples without any presence of secondary

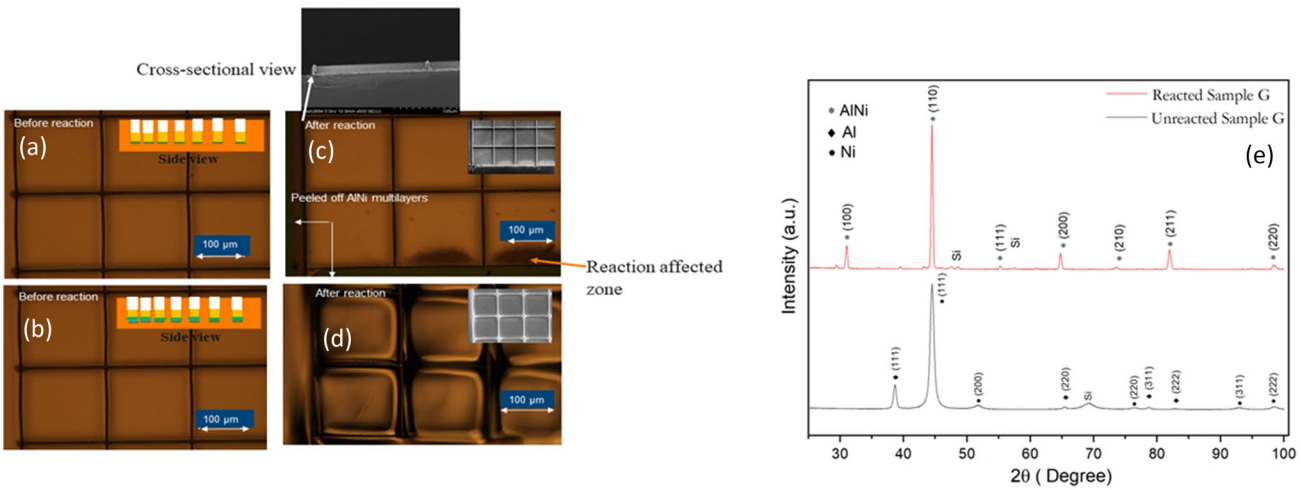

Fig. 4 **a** Microscopy image of the prepared sample F where, T_{total} 5 μm Al/Ni and of the sample F before and **c** after the reaction. **b** Microscopy image of the prepared sample G where, 1 μm PMMA resist were coated on the top of the 1 μm SiO_2 over the prepared etched Si substrate. T_{total} 5 μm Al/Ni were deposited where **d** is the microscopy image after the reaction in sample G. **e** XRD pattern of unreacted and reacted sample G

phase. It indicates that polycrystalline Al/Ni reactive multilayers react and produce AlNi intermetallic compounds from rapid self-propagating exothermic reaction.

Conclusions

The current study shows the effect of the thermal barriers with different sizes in the path of the self-propagating reaction front. This presents a unique opportunity to control the reaction front velocity and emitted temperature by structuring the Al/Ni multilayers. The structuring of the Al/Ni multilayers by lithography is quite a challenging process. In the current study, we optimized the process flow for the fabrication of 5 μm thick Al/Ni multilayers on the Si/SiO_2 substrates. Finally, it is predicted that: (I) The minimum separation of 3 μm between the reactive elements can stop the reaction front; (II) By controlling the heat loss through the substrate via adding less thermal conductive substrates can propagate the reaction front through spaces; (III) Designing the thermal properties of the spaces between the reactive elements enables the modification of the properties of the self-propagating reaction.

Authors contributions Conceptualization, DS and JP; methodology, DS, MS and MB; investigation DS; supervision, JP; review and editing, DS and JP.

Funding Open Access funding enabled and organized by Projekt DEAL. The authors acknowledge the financial support of this research by the German Science Foundation under contract number PE 624/16-1.

Data availability The data that support the findings of this study are available from the corresponding author upon reasonable request.

Declarations

Conflict of interest The authors declare that there is no conflict of interest.

References

1. T. Fujii, T. Namazu, K. Sudoh, S. Sakakihara, S. Inoue, J. Eng. Mater. Technol. **135**, 041002 (2013)
2. T. Fujii, K. Sudoh, S. Sakakihara, M. Naito, S. Inoue, T. Namazu, Jpn. J. Appl. Phys. **52**, 110118 (2013)
3. M.D. Grapes, T.P. Weihs, Combust. Flame **172**, 105 (2016)
4. B. Boettge, J. Braeuer, M. Wiemer, M. Petzold, J. Bagdahn, T. Gessner, J. Micromech. Microeng. **20**, 064018 (2010)
5. J. Braeuer, J, Besser, M. Wiemer, T. Gessner, In Proceedings of the 2011 16th International Solid-State Sensors, Actuators and Microsystems Conference, Beijing, China, 1332 (2011).
6. X. Qiu, R. Tang, R, Liu, S. Guo, H. Yu, In Proceedings of the 2011 16th International Solid-State Sensors, Actuators and Microsystems Conference, Beijing, China, 1665 (2011).
7. J. Braeuer, J, Besser, M. Wiemer, T. Gessner, In Proceedings of the 2012 4th Electronic System-Integration Technology Conference, Amsterdam, The Netherlands, 1 (2012).
8. J. Braeuer, T. Gessner, J. Micromech. Microeng. **24**, 115002 (2014)
9. A. Schumacher, U. Gaiß, S. Knappmann, G. Dietrich, S. Braun, E. Pflug, F. Roscher, K. Vogel, S. Hertel, D. Kähler, In Proceedings of the 2015 European Microelectronics Packaging Conference (EMPC), Friedrichshafen, Germany, 1 (2015).
10. M. Baloochi, D. Shekhawat, S.S. Riegler, S. Matthes, M. Glaser, P. Schaaf, J.P. Bergmann, I. Gallino, J. Pezoldt, Materials **14**, 7815 (2021)
11. J. Braeuer, J. Besser, E. Tomoscheit, D. Klimm, S. Anbumani, M. Wiemer, T. Gessner, ECS Trans. **50**, 241 (2013)
12. J. Braeuer, J. Besser, M. Wiemer, T. Gessner, Sens. Actuators A **188**, 212 (2012)
13. T. Boddington, C.-G. Feng, S.K. Scott, J. Chem. Soc. Faraday Trans. 2 **80**, 973 (1984)
14. B.F. Gray, ANZIAM J. **43**, 1 (2001)
15. S.G. Vadchenko, A.G. Merzhanov, Dokl. Akad. Nauk SSSR **352**, 487 (1997)
16. P.M. Krishenik, A.G. Merzhanov, K.G. Shkadinskii, Combust. Expl. Shock Waves **38**, 313 (2002)
17. S.A. Raskovskiy, G.M. Kumar, S.P. Tewari, Combust. Sci. Technol. **182**, 1009 (2010)
18. F.-D. Tang, A.J. Higgins, S. Goroshin, Combust. Theory Model. **13**, 319 (2009)
19. S.G. Vadchenko, Combust. Expl. Shock Waves **55**, 282 (2019)
20. V.F. Proskudin, V.A. Golubev, P.G. Berezhko, I.E. Boitsov, E.N. Belyaev, V.N. Funin, I.K. Kremzukov, A.Y. Malyshev, Combust. Expl. Shock. Waves **34**, 639 (1998)
21. E.M. Bourim, I.S. Kang, H.Y. Kim, Micromachines **12**, 1272 (2021)
22. T. Namazu, S. Ito, S. Kanetsuki, S. Miyake, Jpn. J. Appl. Phys. **56**, 06GN11 (2017)
23. O.S. Rabinovich, P.S. Grinchuk, M.A. Andreev, B.B. Khina, Physica B **392**, 272 (2007)
24. D.E. Kittel, C.D. Yarrington, M.L. Hobs, M.J. Abere, D.P. Adams, J. Appl. Phys. **123**, 145302 (2018)
25. S. Danzi, M. Menetrey, J. Wohlwend, R. Spolenak, A.C.S. Appl, Mater. Interfaces **11**, 42479 (2019)
26. D. Shekhawat, M. Baloochi, D. Sudhahar, V.A. Raheja, J. Döll, H.O. Jacobs, J. Pezoldt, MRS Adv. **8**, 477 (2023)
27. T.V. Zaporozhets, A.M. Gusak, A.I. Ustinov, Paton Welding J. **2011**(08), 37 (2011)
28. N.A. Manesh, S. Basu, R. Kumar, Combust. Flame **157**, 476 (2010)